

Higgs and SUSY searches at LHC

D P ROY

Department of Theoretical Physics, Tata Institute of Fundamental Research, Homi Bhabha Road, Mumbai 400 005, India

Abstract. I start with a brief introduction to Higgs mechanism and supersymmetry. Then I discuss the theoretical expectations, current limits and search strategies for Higgs boson(s) at LHC – first in the SM and then in the MSSM. Finally I discuss the signatures and search strategies for the superparticles.

Keywords. Supersymmetry; Higgs boson and collider.

PACS Nos 14.80; 12.60; 13.85

1. Introduction

As per the standard model (SM) the basic constituents of matter are the quarks and leptons, which interact by the exchange of gauge bosons – photon, gluon and the massive W and Z bosons. By now we have seen all the quarks and leptons as well as the gauge bosons. But the story is not complete yet because of the mass problem.

2. Mass problem (Higgs mechanism)

The question is how to give mass to the weak gauge bosons, W and Z , without breaking gauge symmetry, which is required for a renormalisable field theory. In order to appreciate it consider the weak interaction Lagrangian of a charged scalar field ϕ ; i.e.

$$\mathcal{L} = \left(\partial_\mu \phi + ig \frac{\vec{\tau}}{2} \vec{W}_\mu \phi \right)^\dagger \left(\partial_\mu \phi + ig \frac{\vec{\tau}}{2} \vec{W}_\mu \phi \right) - [\mu^2 \phi^\dagger \phi + \lambda (\phi^\dagger \phi)^2] - \frac{1}{4} \vec{W}_{\mu\nu} \vec{W}_{\mu\nu}, \quad (1)$$

where

$$\vec{W}_{\mu\nu} = \partial_\mu \vec{W}_\nu - \partial_\nu \vec{W}_\mu - g \vec{W}_\mu \times \vec{W}_\nu \quad (2)$$

is the field tensor for the weak gauge bosons \vec{W}_μ . The charged and the neutral W bosons form a $SU(2)$ vector, reflecting the nonabelian nature of this gauge group. This is responsible for the last term in (2), which leads to gauge boson self-interaction. Correspondingly the gauge transformation on \vec{W}_μ has an extra term, i.e.

$$\phi \rightarrow e^{i\vec{\alpha} \cdot \vec{\tau}} \phi, \quad \vec{W}_\mu \rightarrow \vec{W}_\mu - \frac{1}{g} \partial_\mu \vec{\alpha} - \vec{\alpha} \times \vec{W}_\mu. \quad (3)$$

This ensures gauge invariance of $\vec{W}_{\mu\nu}$, and hence for the last term of the Lagrangian, representing gauge boson kinetic energy and self-interaction. Evidently the middle term, representing scalar mass and self-interaction, is invariant under gauge transformation on ϕ . Finally the first term, representing scalar kinetic energy and gauge interaction, can be easily shown to be invariant under the simultaneous gauge transformations (3). However the addition of a mass term

$$-M^2 \vec{W}_\mu \cdot \vec{W}_\mu, \quad (4)$$

would clearly break the gauge invariance of the Lagrangian. Note that, in contrast the scalar mass term, $\mu^2 \phi^\dagger \phi$, is clearly gauge invariant. This phenomenon is exploited to give mass to the gauge bosons through back door without breaking the gauge invariance of the Lagrangian. This is the celebrated Higgs mechanism of spontaneous symmetry breaking [1].

One starts with a $SU(2)$ doublet of complex scalar field ϕ with imaginary mass, i.e. $\mu^2 < 0$. Consequently the minimum of the scalar potential, $\mu^2 \phi^\dagger \phi + \lambda(\phi^\dagger \phi)^2$, moves out from the origin to a finite value

$$v = \sqrt{-\mu^2/\lambda}, \quad (5)$$

i.e. the field develops a finite vacuum expectation value. Since the quantum perturbative expansion is stable only around a local minimum, one has to translate the field by the constant quantity,

$$\phi = v + H(x). \quad (6)$$

Thus one gets a valid perturbative field theory in terms of the redefined field H . This represents the physical Higgs boson, while the 3 other components of the complex doublet field are absorbed to give mass and hence longitudinal components to the gauge bosons.

Substituting (6) in the first term of the Lagrangian (1) leads to a mass term for W ,

$$M_W = \frac{1}{2} g v. \quad (7)$$

It also leads to a HWW coupling,

$$\frac{1}{2} g^2 v = g M_W, \quad (8)$$

i.e. the Higgs coupling to the gauge bosons is proportional to the gauge boson mass. Similarly its couplings to quarks and leptons can be shown to be proportional to their respective masses, i.e.

$$h_{\ell,q} = m_{\ell,q}/v = \frac{1}{2} g m_{\ell,q}/M_W. \quad (9)$$

Indeed, this is the source of the fermion masses in the SM. Finally substituting (6) in the middle term of the Lagrangian leads to a real mass for the physical Higgs boson,

$$M_H = v\sqrt{2\lambda} = M_W(2\sqrt{2\lambda}/g). \quad (10)$$

Substituting $M_W = 80$ GeV and $g = 0.65$ along with a perturbative limit on the scalar self-coupling $\lambda \lesssim 1$, implies that the Higgs boson mass is bounded by $M_H < 1000$ GeV. But the

story does not end here. Giving mass to the gauge bosons via the Higgs mechanism leads to the so-called hierarchy problem.

3. Hierarchy problem (supersymmetry)

The problem is how to peg down the Higgs scalar in the desired mass range of a few hundred GeV. This is because the scalar masses are known to have quadratically divergent quantum corrections from radiative loops involving e.g. quarks or leptons. These would push the output scalar mass to the cut-off scale of the SM, i.e. the GUT scale (10^{16} GeV) or the Planck scale (10^{19} GeV). The desired mass range of $\sim 10^2$ GeV is clearly tiny compared to these scales. This is the so-called hierarchy problem. The underlying reason for the quadratic divergence is that the scalar masses are not protected by any symmetry unlike the fermion and the gauge boson masses, which are protected by chiral symmetry and gauge symmetry. Of course it was this very property of the scalar mass that was exploited to give masses to the fermions and gauge bosons in the first place. Therefore it can not be simply wished away.

The most attractive solution to this problem is provided by supersymmetry (SUSY), a symmetry between fermions and bosons [2]. It predicts the quarks and leptons to have scalar superpartners called squarks and sleptons ($\tilde{q}, \tilde{\ell}$), and the gauge bosons to have fermionic superpartners called gauginos ($\tilde{g}, \tilde{\gamma}, \tilde{W}, \tilde{Z}$). In the minimal supersymmetric extension of the standard model (MSSM) one needs two Higgs doublets $H_{1,2}$, with opposite hypercharge $Y = \pm 1$, to give masses to the up and down type quarks. The corresponding fermionic superpartners are called Higgsinos ($\tilde{H}_{1,2}$). The opposite hypercharge of these two sets of fermions ensures anomaly cancellation.

SUSY ensures that the quadratically divergent quantum corrections from quark and lepton loops are cancelled by the contributions from the corresponding squark and slepton loops. Thus the Higgs masses can be kept in the desired range of $\sim 10^2$ GeV. However this implies two important constraints on SUSY breaking.

- (i) SUSY can be broken in masses but not in couplings (soft breaking), so that the coefficients of the cancelling contributions remain equal and opposite.
- (ii) The size of SUSY breaking in masses is $\sim 10^2$ GeV, so that the size of the remainder remains within this range. Thus the superpartners of the SM particles are also expected to lie in the mass range of $\sim 10^2$ GeV, going up to 1000 GeV.

4. SM Higgs boson: Theoretical constraints and search strategy

The Higgs self coupling λ is ultra-violet divergent. It evolves according to the renormalisation group equation (RGE)

$$\frac{d\lambda}{d \ln(\mu/M_W)} = \frac{3\lambda^2}{2\pi^2}. \quad (11)$$

It can be easily solved to give

$$\lambda(\mu) = \frac{1}{1/\lambda(M_W) - (3/2\pi^2) \ln(\mu/M_W)}, \quad (12)$$

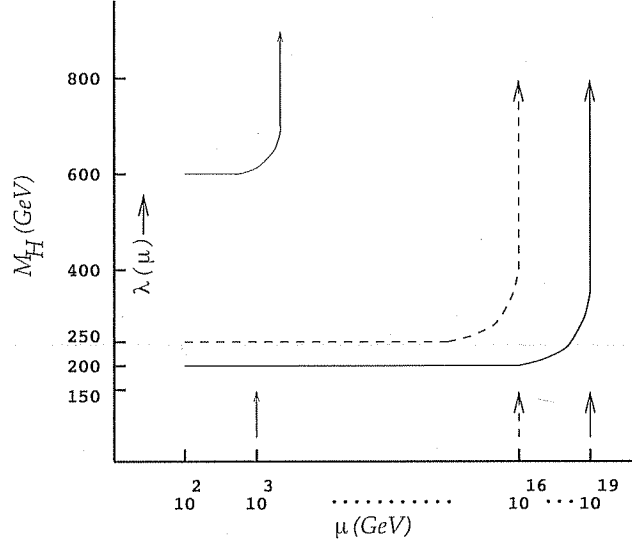


Figure 1. The triviality bounds on the Higgs boson mass corresponding to different cut-off scales, i.e. TeV, GUT and Planck scales.

which has a Landau pole at

$$\begin{aligned} \mu_\infty &= M_W e^{2\pi^2/3\lambda(M_W)}, \\ \lambda(M_W) &= \frac{g^2 M_H^2}{8 M_W^2}. \end{aligned} \quad (13)$$

Thus the larger the starting value $\lambda(M_W)$, the sooner will the coupling diverge. This is illustrated in figure 1. Evidently the theory is valid only up to a cut-off scale $\Lambda = \mu_\infty$. Requiring the theory to be valid at all energies, $\Lambda \rightarrow \infty$, would imply $\lambda(M_W) \rightarrow 0$; i.e. the only good $\lambda\phi^4$ theory is a trivial theory. Surely we do not want that. But if we want the theory to be valid up to the Planck scale or GUT scale, we must have a relatively small $\lambda(M_W)$, which corresponds to a small $M_H \lesssim 200$ GeV. If on the other hand we assume it to be valid only up to the TeV scale, then we can have a larger $\lambda(M_W)$, corresponding to a relatively large $M_H \lesssim 600$ GeV. This is the so-called triviality bound [3]. If M_h is significantly larger than 600 GeV, then the range of validity of the theory is limited to $\Lambda < 2M_H$. This would correspond to a composite Higgs scenario, e.g. technicolour models.

Figure 2 shows the triviality bound on the Higgs mass against the cut-off scale Λ of the theory [4]. It also shows a lower bound on the Higgs mass, which comes from a negative contribution to the RGE (11) from the top Yukawa coupling, i.e.

$$\frac{d\lambda}{d\ln(\mu/M_W)} = \frac{3}{2\pi^2} (\lambda^2 + \lambda h_t^2 - h_t^4). \quad (14)$$

The Yukawa coupling being ultra-violet divergent turns λ negative at a high energy scale; and the smaller the starting value of λ (or equivalently M_H) the sooner will it become

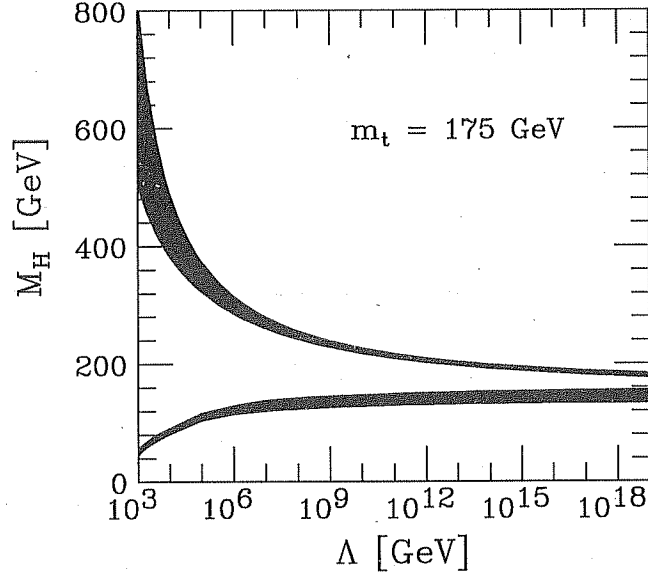


Figure 2. The upper and lower bounds on the mass of the SM Higgs boson as functions of the cut-off scale [4].

negative. A negative λ coupling has the undesirable feature of an unstable vacuum (eq. (5)). Thus one can define a cut-off scale Λ for the theory, where this change of sign occurs. The lower curve of figure 2 shows the lower bound on M_H as a function of the cut-off scale Λ including the theoretical uncertainty [5]. We see from this figure that the longer the range of validity of the theory, the stronger will be the upper and lower bounds on M_H . Thus assuming no new physics up to the GUT or Planck scale (the desert scenario) would constrain the SM Higgs mass to lie in the range

$$M_H = 130\text{--}190 \text{ GeV}. \quad (15)$$

However the lower bound becomes invalid once we have more than one Higgs doublet, since the unique relation between the top mass and Yukawa coupling (9) will no longer hold. In particular, one expects an upper bound of ~ 130 GeV for the lightest Higgs boson mass in MSSM instead of a lower bound, as we shall see below. Since one needs SUSY or some other form of new physics to stabilize the Higgs mass, the above vacuum stability bound may have limited significance. Nonetheless it is interesting to note that the predicted range of the SM Higgs boson mass (15) agrees favourably with the indirect estimate of this quantity from the precision measurement of electro-weak parameters at LEP/SLD [6], i.e.

$$M_H = 115^{+116}_{-66} \text{ GeV} (< 420 \text{ GeV at 95\% CL}). \quad (16)$$

It should be added however that there is a lingering discrepancy between the LEP and the SLD values of $\sin^2 \theta_W$, which could affect the central value and the 95% CL limit of M_H appreciably. Thus all one can say at the moment is that these indirect estimates are consistent with a relatively light Higgs boson.

D P Roy

The search strategy for Higgs boson is based on its preferential coupling to the heavy quarks and gauge bosons as seen from (8,9). The LEP-I search was based on the so-called Bjorken process

$$e^+e^- \rightarrow Z \rightarrow HZ^* \rightarrow \bar{b}b(\ell^+\ell^-, \nu\nu, \bar{q}q), \quad (17)$$

while the LEP-II search is based on the associated process with Z and Z^* interchanged. The current LEP-II limit from the preliminary ALEPH data at 183 GeV is [7]

$$M_H > 88.6 \text{ GeV}. \quad (18)$$

The forthcoming runs at 192–200 GeV are expected to extend the search upto

$$M_H = 95\text{--}100 \text{ GeV}. \quad (19)$$

Thus the Higgs mass range of interest to LHC is $M_H \gtrsim 90$ GeV. Figure 3 shows the total decay width of the Higgs boson over this range along with the branching ratios for the important decay channels [8]. It is clear from this figure that the mass range can be divided into two parts – (a) $M_H < 2M_W$ (90–160 GeV) and (b) $M_H > 2M_W$ (160–1000 GeV).

The first part is the so-called intermediate mass region, where the Higgs width is expected to be only a few MeV. The dominant decay mode is $H \rightarrow \bar{b}b$. This has unfortunately a huge QCD background, which is ~ 1000 times larger than the signal. By far the cleanest channel is $\gamma\gamma$, where the continuum background is a 2nd order EW process. However, the signal suffers from a small branching ratio

$$B(H \rightarrow \gamma\gamma) \sim 1/1000, \quad (20)$$

since it is a higher order process, induced by the top quark loop. So one needs a very high jet/ γ rejection factor $\gtrsim 10^8$. Besides the continuum background being proportional to $\Delta M_{\gamma\gamma}$, one needs a high resolution,

$$\Delta M_{\gamma\gamma} \lesssim 1 \text{ GeV i.e. } \lesssim 1\% \text{ of } M_H. \quad (21)$$

This requires fine EM calorimetry, capable of measuring the γ energy and direction to 1% accuracy. In this respect CMS is expected to do better than ATLAS. The projected Higgs mass reach of the two detectors via this channel are $M_H = 90\text{--}140$ GeV (CMS) and $110\text{--}140$ GeV (ATLAS) at the high luminosity run of LHC (100 fb^{-1}).

One can get a feel for the size of the signal from the Higgs production cross-sections shown in figure 4. The relevant production processes are

$$gg \xrightarrow{\bar{t}t^*} H, \quad (22)$$

$$qq \xrightarrow{W^*W^*} Hqq, \quad (23)$$

$$q\bar{q}' \xrightarrow{W^*} HW, \quad (24)$$

$$gg, q\bar{q} \rightarrow H\bar{t}t(H\bar{b}b). \quad (25)$$

The largest cross-section, coming from gluon–gluon fusion via the top quark loop (22), is of the order of 10 pb. Thus the expected size of the $H \rightarrow \gamma\gamma$ signal is ~ 10 fb, corresponding to $\sim 10^3$ events. The estimated continuum background is $\sim 10^4$ events, which can of course be subtracted out. Thus the significance of the signal is given by its relative size with respect to the statistical uncertainty in the background, i.e.

$$S/\sqrt{B} \simeq 10. \quad (26)$$

Higgs and SUSY searches at LHC

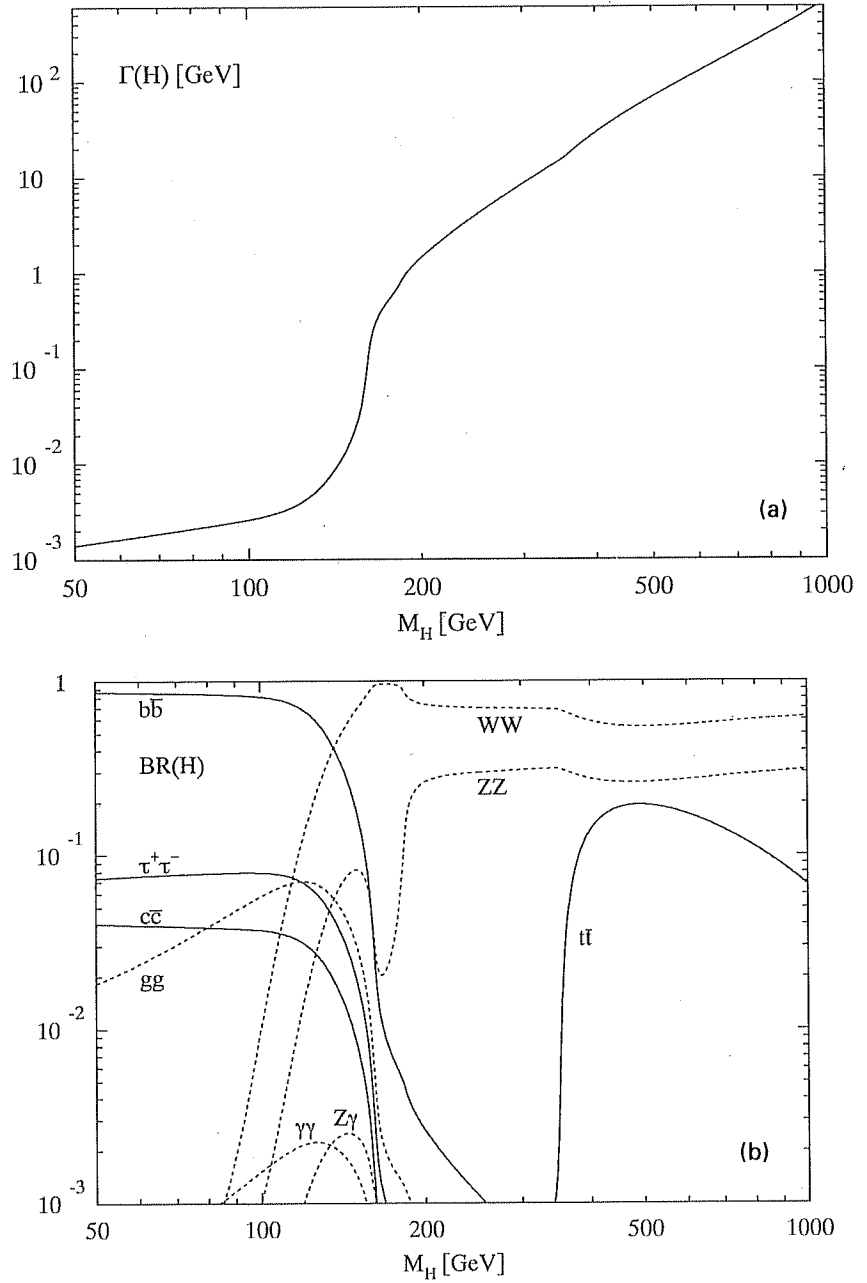


Figure 3. Total decay width and the main branching ratios of the SM Higgs boson [8].

By far the cleanest signal is provided by the associated Bjorken process (24), with a cross-section of ~ 1 fb in the $H \rightarrow \gamma\gamma$ channel. Combining this with the BR of 2/9 for $W \rightarrow \ell\nu$ implies a signal of 20–30 events in the $\ell + \gamma\gamma$ channel. While the signal size is admittedly

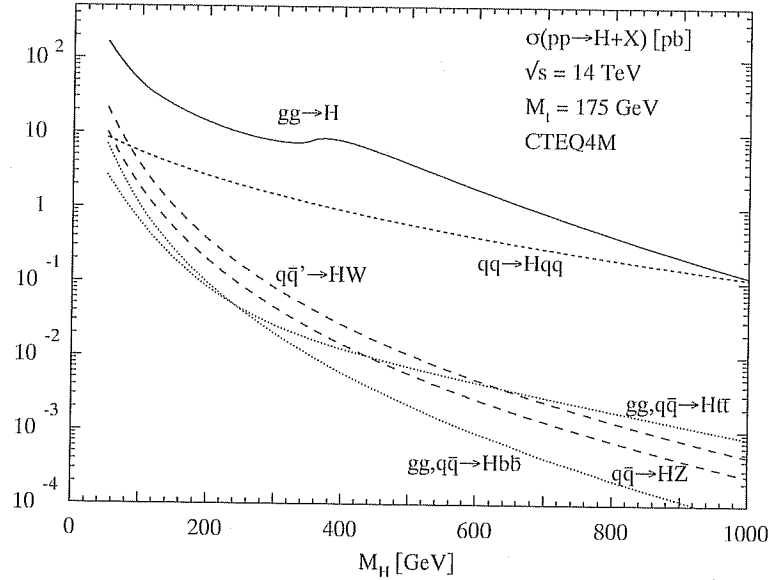


Figure 4. Production cross-sections of the SM Higgs boson at LHC [8].

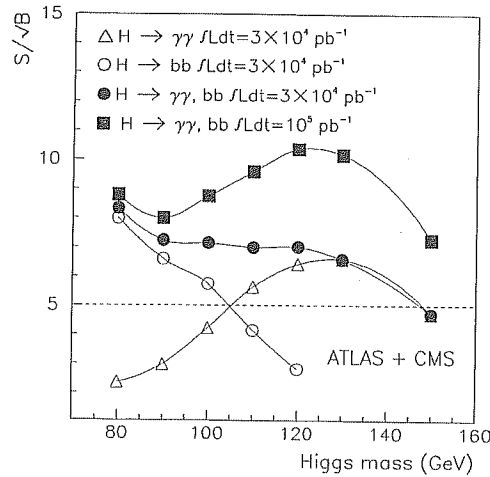


Figure 5. The expected significance level of the SM Higgs signal at LHC over the intermediate mass region [9].

small, the estimated background is only ~ 10 events. Thus the S/\sqrt{B} ratio is again ~ 10 . Detailed signal and background simulations for these channels can be found in [9]. The result is summarized in figure 5. It shows that one expects a 5σ signal up to a Higgs mass of 150 GeV for an integrated luminosity of 30 fb^{-1} . This corresponds to the low luminosity run of LHC over the first 3 years. It may be noted that the dominant decay channel, $H \rightarrow b\bar{b}$, can be important for Higgs search below 100 GeV. It comes from the associated

Higgs and SUSY searches at LHC

Bjorken process (24), where the leptonic decay of the accompanying $W(Z)$ helps to reduce the background. However this region should be already covered by LEP-II.

For higher masses the most promising Higgs decay channel is

$$H \rightarrow ZZ \rightarrow \ell^+ \ell^- \ell^+ \ell^-, \quad (27)$$

since reconstruction of the $\ell^+ \ell^-$ invariant masses makes it practically background free. Thus it provides the most important Higgs signal right from the sub-threshold region of $M_H = 140$ GeV up to 600 GeV (see figure 3). Note however a sharp dip in the ZZ branching ratio at $M_H = 160$ –170 GeV due to the opening of the WW channel. The most important Higgs signal in this dip region is expected to come from [10]

$$H \rightarrow WW \rightarrow \ell^+ \nu \ell^- \bar{\nu}. \quad (28)$$

However in general this channel suffers from a much larger background for two reasons – (i) it is not possible to reconstruct the W masses because of the two neutrinos and (ii) there is a large WW background from $t\bar{t}$ decay.

For large Higgs mass, $M_H = 600$ –1000 GeV, the 4-lepton signal (27) becomes too small in size. In this case the decay channels

$$H \rightarrow WW \rightarrow \ell \nu q \bar{q}', \quad H \rightarrow ZZ \rightarrow \ell^+ \ell^- q \bar{q}, \quad (29)$$

are expected to provide more favourable signals. The biggest background comes from single $W(Z)$ production along with QCD jets. However, one can exploit the fact that a large part of the signal cross-section in this case comes from WW fusion (23), which is accompanied by two forward (large-rapidity) jets. One can use the double forward jet tagging to effectively control the background. Indeed simulation studies by the CMS and ATLAS collaborations show that using this strategy one can extend the Higgs search right up to 1000 GeV[9].

5. MSSM Higgs bosons: Theoretical constraints and search strategy

As mentioned earlier, the MSSM contains two Higgs doublets, which correspond to 8 independent states. After 3 of them are absorbed by the W and Z bosons, one is left with 5 physical states: two neutral scalars h^0 and H^0 , a pseudoscalar A^0 , and a pair of charged Higgs scalars H^\pm . At the tree-level their masses and couplings are determined by only two parameters – the ratio of the two vacuum expectation values, $\tan \beta$, and one of the scalar masses, usually taken to be M_A . However, the neutral scalars get a large radiative correction from the top quark loop along with the top squark (stop) loop. To a good approximation this is given by [11]

$$\epsilon = \frac{3g^2 m_t^4}{8\pi^2 M_W^2} \ln \left(\frac{M_{\tilde{t}}^2}{m_t^2} \right), \quad (30)$$

plus an additional contribution from the $\tilde{t}_{L,R}$ mixing,

$$\epsilon_{\text{mix}} = \frac{3g^2 m_t^4}{8\pi^2 M_W^2} \frac{A_t^2}{M_{\tilde{t}}^2} \left(1 - \frac{A_t^2}{12M_{\tilde{t}}^2} \right) \leq \frac{9g^2 m_t^4}{8\pi^2 M_W^2}. \quad (31)$$

Thus while the size of ϵ_{mix} depends on the trilinear SUSY breaking parameter A_t , it has a maximum value independent of A_t . As expected the radiative corrections vanish in the exact SUSY limit. One can estimate the rough magnitude of these corrections assuming a SUSY breaking scale of $M_{\tilde{t}} = 1$ TeV. The leading log QCD corrections can be taken into account by using the running mass of top at the appropriate energy scale [11]; i.e. $m_t(\sqrt{m_t M_{\tilde{t}}}) \simeq 157$ GeV in (30) and $m_t(M_{\tilde{t}}) \simeq 150$ GeV in (31) instead of the top pole mass of 175 GeV. One can easily check that the resulting size of the radiative corrections are

$$\epsilon \sim M_W^2 \quad \text{and} \quad 0 < \epsilon_{\text{mix}} \lesssim M_W^2. \quad (32)$$

The neutral scalar masses are obtained by diagonalizing the mass-squared matrix

$$\begin{pmatrix} M_A^2 \sin^2 \beta + M_Z^2 \cos^2 \beta & -(M_A^2 + M_Z^2) \sin \beta \cos \beta \\ -(M_A^2 + M_Z^2) \sin \beta \cos \beta & M_A^2 \cos^2 \beta + M_Z^2 \sin^2 \beta + \epsilon' \end{pmatrix} \quad (33)$$

with $\epsilon' = (\epsilon + \epsilon_{\text{mix}}) / \sin^2 \beta$. Thus

$$\begin{aligned} M_h^2 &= \frac{1}{2} [M_A^2 + M_Z^2 + \epsilon' - \{(M_A^2 + M_Z^2 + \epsilon')^2 - 4M_A^2 M_Z^2 \cos^2 \beta \\ &\quad - 4\epsilon' (M_A^2 \sin^2 \beta + M_Z^2 \cos^2 \beta)\}^{1/2}] \\ M_H^2 &= M_A^2 + M_Z^2 + \epsilon' - M_h^2 \\ M_{H^\pm}^2 &= M_A^2 + M_W^2 \end{aligned} \quad (34)$$

where h denotes the lighter neutral scalar [12]. One can easily check that its mass has an upper bound for $M_A \gg M_Z$, i.e.

$$M_h^2 \rightarrow M_Z^2 \cos^2 2\beta + \epsilon + \epsilon_{\text{mix}}, \quad (35)$$

while $M_H^2, M_{H^\pm}^2 \rightarrow M_A^2$. Thus the MSSM contains at least one light Higgs boson h , whose tree-level mass limit $M_h < M_Z$, goes up to 130–140 GeV after including the radiative corrections. Figure 6 shows the masses of the MSSM Higgs bosons against M_A for two representative values of $\tan \beta = 1.5$ and 30. The predictions without stop mixing and with maximal mixing are shown in separate plots. Note that the h mass limit is particularly strong in the low $\tan \beta$ (~ 1) region, i.e. $M_h < 80$ –100 GeV depending on the size of stop mixing parameter A_t . Consequently the low $\tan \beta$ region is particularly susceptible to the ongoing Higgs search at LEP-II as we shall see below.

Let us consider now the couplings of the MSSM Higgs bosons. A convenient parameter for this purpose is the mixing angle α between the neutral scalars, i.e.

$$\tan 2\alpha = \tan 2\beta \frac{M_A^2 + M_Z^2}{M_A^2 - M_Z^2 + \epsilon' / \cos 2\beta}, \quad -\pi/2 < \alpha < 0. \quad (36)$$

Note that

$$\alpha \xrightarrow{M_A \gg M_Z} \beta - \pi/2. \quad (37)$$

Table 1 shows the important couplings of the neutral Higgs bosons relative to those of the SM Higgs boson. The limiting values of these couplings at large M_A are indicated by arrows. The corresponding couplings of the charged Higgs boson, which has no SM

Higgs and SUSY searches at LHC

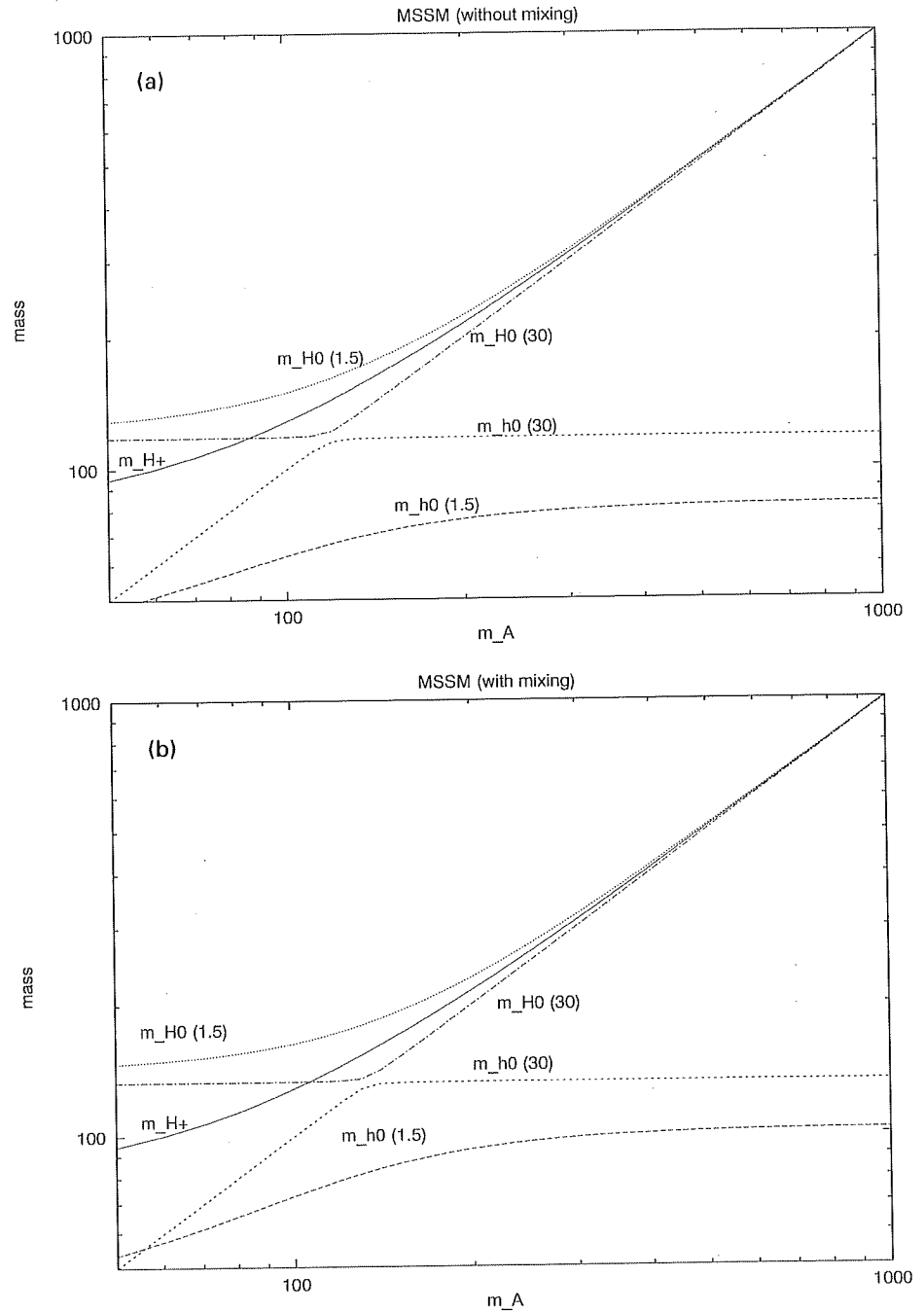


Figure 6. Masses of the MSSM Higgs boson h^0 , H^0 and H^\pm as functions of the pseudoscalar mass for $\tan\beta = 1.5$ and 30. The predictions without and with maximal stop mixing are shown separately.

D P Roy

Table 1. Important couplings of the MSSM Higgs bosons h , H and A relative to those of the SM Higgs boson.

Channel	H_{SM}	h	H	A
$\bar{b}b(\tau^+\tau^-)$	$\frac{gm_b}{2M_W}(m_\tau)$	$\sin \alpha / \cos \beta$ $\rightarrow 1$	$\cos \alpha / \cos \beta$ $\tan \beta$	$\tan \beta$ "
$\bar{t}t$	$g \frac{m_t}{2M_W}$	$\cos \alpha / \sin \beta$ $\rightarrow 1$	$\sin \alpha / \sin \beta$ $\cot \beta$	$\cot \beta$ "
$WW(ZZ)$	$gM_W(M_Z)$	$\sin(\beta - \alpha)$ $\rightarrow 1$	$\cos(\beta - \alpha)$ 0	0 "

analogue, are

$$H^+\bar{t}b : \frac{g}{\sqrt{2}M_W}(m_t \cot \beta + m_b \tan \beta), \quad H^+\tau\nu : \frac{g}{\sqrt{2}M_W}m_\tau \tan \beta,$$

$$H^+W^-Z : 0. \quad (38)$$

Note that the top Yukawa coupling is ultraviolet divergent. Assuming it to lie within the perturbation theory limit all the way upto the GUT scale implies

$$1 < \tan \beta < m_t/m_b, \quad (39)$$

which is therefore the favoured range of $\tan \beta$. However, it assumes no new physics beyond the MSSM up to the GUT scale, which is a stronger assumption than MSSM itself. Nonetheless we shall concentrate in this range.

Coming back to the neutral Higgs couplings of table 1, we see that in the large M_A limit the light Higgs boson (h) couplings approach the SM values. The other Higgs bosons are not only heavy, but their most important couplings are also suppressed. This is the so-called decoupling limit, where the MSSM Higgs sector is phenomenologically indistinguishable from the SM. It follows therefore that the Higgs search strategy for $M_A \gg M_Z$ should be the same as the SM case, i.e. via

$$h \rightarrow \gamma\gamma. \quad (40)$$

At lower M_A , several of the MSSM Higgs bosons become light. Unfortunately their couplings to the most important channels, $\bar{t}t$ and WW/ZZ , are suppressed relative to the SM Higgs boson [12]. Thus their most important production cross-sections as well as their decay BRs into the $\gamma\gamma$ channel are suppressed relative to the SM case. Consequently the Higgs detection in this region is very hard and it calls for multiprong strategy from the three sides in the $M_A - \tan \beta$ plane (figure 7): (a) low M_A , (b) high $\tan \beta$ and (c) low $\tan \beta$.

(a) Low $M_A (\lesssim M_Z)$: In this case $M_{H^\pm} < M_t$; and the best strategy is to search for H^\pm in top quark decay, i.e.

$$t \rightarrow bH^+, \quad H^+ \rightarrow \tau\nu, \quad (41)$$

via preferential top decay into the τ channel as well as the opposite polarization of τ with respect to the SM decay ($W \rightarrow \tau\nu$) [14].

(b) High $\tan \beta (\sim m_t/m_b)$: It is clear from table 1 that in this case the best production and

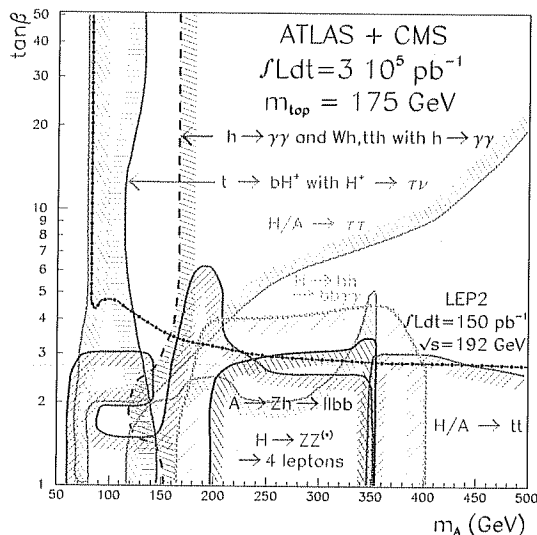


Figure 8. Regions of the parameter space ($M_A - \tan\beta$) covered by the 5σ discovery contours of various MSSM Higgs signals from the combined ATLAS + CMS experiments after 3 years of high luminosity run of LHC [17].

limits. Moreover the LEP-II limit will go down to a lower range of $\tan\beta$ when stop mixing effect is taken into account (figure 6). This will enlarge the size of the hole further. Finally, figure 8 shows that it would be possible to close the hole if one combines the CMS and the ATLAS data collected over an integrated luminosity of 300 fb^{-1} [17]. This corresponds to 3 years of high luminosity run of LHC; and illustrates the challenge involved in the search for the MSSM Higgs bosons. Note that even in this case there is a large region where one would see only one Higgs boson (h) with SM like couplings and hence not be able to distinguish the SUSY from the SM Higgs sector. Fortunately it will be possible and in fact much easier to probe SUSY directly via superparticle search as we see below.

6. Superparticles: Signature and search strategy

I shall concentrate on the standard SUSY model, where the superparticle signature is based on R -parity conservation. Let me start therefore with a brief discussion of R -parity. The presence of scalar quarks in SUSY can lead to baryon and lepton number violating interactions of the type $ud \rightarrow \bar{s}$ and $\bar{s} \rightarrow e^+ \bar{u}$, i.e.

$$ud \xrightarrow{\bar{s}} e^+ \bar{u}. \tag{43}$$

Moreover adding a spectator u quark to both sides one sees that this can lead to a catastrophic proton decay, i.e.

$$p(uud) \xrightarrow{\bar{s}} e^+ \pi^0 (\bar{u}u). \tag{44}$$

Higgs and SUSY searches at LHC

Since the superparticle masses are assumed to be of the order M_W for solving the hierarchy problem, this would imply a proton life time similar to the typical weak decay time of $\sim 10^{-8}$ sec! The best way to avoid this catastrophic proton decay is via R -parity conservation, where

$$R = (-1)^{3B+L+2S} \quad (45)$$

is defined to be +1 for the SM particles and -1 for their superpartners, since they differ by $1/2$ unit of spin S . It automatically ensures L and B conservation by preventing single emission (absorption) of superparticle.

Thus R -conservation implies that (i) superparticles are produced in pair and (ii) the lightest superparticle (LSP) is stable. Astrophysical evidences against such a stable particle carrying colour or electric charge imply that the LSP is either sneutrino $\tilde{\nu}$ or photino $\tilde{\gamma}$ (or in general the lightest neutralino). The latter alternative is favoured by the present SUSY models. In either case the LSP is expected to have only weak interaction with ordinary matter like the neutrino, since e.g.

$$\tilde{\gamma}q \xrightarrow{\tilde{q}} q\tilde{\gamma} \quad \text{and} \quad \nu q \xrightarrow{W} e q' \quad (46)$$

have both electroweak couplings and $M_{\tilde{q}} \sim M_W$. This makes the LSP an ideal candidate for the cold dark matter. It also implies that the LSP would leave the normal detectors without a trace like the neutrino. The resulting imbalance in the visible momentum constitutes the canonical missing transverse-momentum (\cancel{p}_T) signature for superparticle production at hadron colliders. It is also called the missing transverse-energy (\cancel{E}_T) as it is often measured as a vector sum of the calorimetric energy deposits in the transverse plane.

The main processes of superparticle production at LHC are the QCD processes of quark-antiquark and gluon-gluon fusion [18]

$$q\bar{q}, gg \rightarrow \tilde{q}\bar{\tilde{q}}(\tilde{g}\tilde{g}). \quad (47)$$

The NLO corrections can increase these cross-sections by 15–20% [19]. The simplest decay processes for the produced squarks and gluinos are

$$\tilde{q} \rightarrow q\tilde{\gamma}, \quad \tilde{g} \rightarrow q\bar{q}\tilde{\gamma}. \quad (48)$$

Convoluting these with the pair production cross-sections (47) gives the simplest jets + \cancel{p}_T signature for squark/gluino production, which were adequate for the early searches for relatively light squarks and gluinos. However, over the mass range of current interest (≥ 100 GeV) the cascade decays of squark and gluino into the LSP via the heavier chargino/neutralino states are expected to dominate over the direct decays (48). This is both good news and bad news. On the one hand the cascade decay degrades the missing- p_T of the canonical jets + \cancel{p}_T signature. But on the other hand it gives a new multilepton signature via the leptonic decays of these chargino/neutralino states. It may be noted here that one gets a mass limit of

$$M_{\tilde{q},\tilde{g}} > 180 \text{ GeV} \quad (49)$$

from the Tevatron data using either of the two signatures [20].

The cascade decay is described in terms of the $SU(2) \times U(1)$ gauginos $\tilde{W}^{\pm,0}, \tilde{B}^0$ along with the Higgsinos $\tilde{H}^{\pm}, \tilde{H}_1^0$ and \tilde{H}_2^0 . The \tilde{B} and \tilde{W} masses are denoted by M_1 and M_2 respectively while the Higgsino masses are functions of the supersymmetric Higgsino

D P. Roy

mass parameter μ and $\tan\beta$. The charged and the neutral gauginos will mix with the corresponding Higgsinos to give the physical chargino $\chi_{1,2}^\pm$ and neutralino $\chi_{1,2,3,4}^0$ states. Their masses and compositions can be found by diagonalizing the corresponding mass matrices, i.e.

$$M_C = \begin{pmatrix} M_2 & \sqrt{2}M_W \sin\beta \\ \sqrt{2}M_W \cos\beta & \mu \end{pmatrix},$$

$$M_N = \begin{pmatrix} M_1 & 0 & -M_Z \sin\theta_W \cos\beta & M_Z \sin\theta_W \sin\beta \\ 0 & M_2 & M_Z \cos\theta_W \cos\beta & -M_Z \cos\theta_W \sin\beta \\ -M_Z \sin\theta_W \cos\beta & M_Z \cos\theta_W \cos\beta & 0 & -\mu \\ M_Z \sin\theta_W \sin\beta & -M_Z \cos\theta_W \sin\beta & -\mu & 0 \end{pmatrix}. \quad (50)$$

Let me try to present a simplified picture. Assuming unification of the $SU(3) \times SU(2) \times U(1)$ gaugino masses at the GUT scale the RGE relates the corresponding masses at the low energy scale ($\sim 10^2$ GeV) to the respective gauge couplings. Thus

$$M_2 = (g^2/g_S^2)M_{\tilde{g}} \simeq 0.3M_{\tilde{g}}$$

$$M_1 = (5 \tan^2 \theta_W/3)M_2 \simeq 0.5M_2. \quad (51)$$

Moreover the SUGRA assumptions of a common scalar mass at the GUT scale along with the radiative breaking of the EW symmetry (5), imply

$$\mu \gg M_2. \quad (52)$$

It is clear from (50)–(52) that the lighter chargino and neutralino states are expected to be dominated by gaugino components. In particular

$$\chi_{1,2}^\pm \simeq \tilde{W}^\pm, \tilde{H}^\pm$$

$$\chi_{1,2,\dots}^0 \simeq \tilde{B}, \tilde{W}^0, \dots \quad (53)$$

With the above systematics one can understand the essential features of cascade decay. For illustration I shall briefly discuss cascade decay of gluino for two representative gluino mass regions of interest to LHC.

(i) $M_{\tilde{g}} \simeq 300$ GeV: In this case the gluino decays into the light quarks

$$g \rightarrow \bar{q}q[\tilde{B}(0.2), \tilde{W}^0(0.3), \tilde{W}^\pm(0.5)], \quad q \neq t, \quad (54)$$

which have negligible Yukawa couplings. Thus the decay branching ratios are proportional to the squares of the respective gauge couplings as indicated in parantheses. Because of the smaller $U(1)$ gauge coupling relative to the $SU(2)$, the direct decay into the LSP (\tilde{B}) is small compared to cascade decay via the heavier (\tilde{W} dominated) chargino and neutralino states. The latter decay into the LSP via real or virtual W/Z emission,

$$\tilde{W}_0 \rightarrow Z\tilde{B} \rightarrow \ell^+ \ell^- \tilde{B}(0.06), \tilde{W}^\pm \rightarrow W\tilde{B} \rightarrow \ell^\pm \nu \tilde{B}(0.2), \quad (55)$$

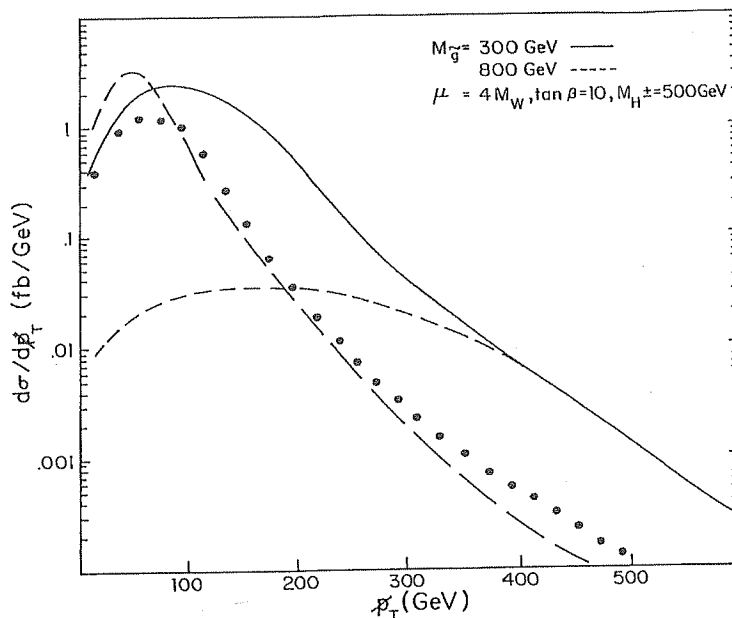


Figure 9. The expected size of the LSD signals for 300 and 800 GeV gluino production at LHC are shown against the accompanying missing- p_T . The real and fake LSD backgrounds from $\bar{t}t$ production are shown by long dashed and dotted lines respectively [21].

whose leptonic branching ratios are indicated in parantheses. From (54) and (55) one can easily calculate the branching ratios of dilepton and trilepton states resulting from the decay of a gluino pair. In particular the dilepton final state via the charginos has a branching ratio of 1%. Then the Majorana nature of \tilde{g} implies a distinctive like sign dilepton (LSD) signal with a BR of $\sim 1/2\%$.

(ii) $\tilde{M}_{\tilde{g}} \gtrsim 500$ GeV: In this case the large top Yukawa coupling implies a significant decay rate via

$$\tilde{g} \rightarrow t\bar{b}\tilde{H}^-, \quad (56)$$

where both t and \tilde{H}^- can contribute to the leptonic final state via

$$t \rightarrow bW^+ \rightarrow b\ell^+\nu(0.2), \quad \tilde{H}^- \rightarrow W^-\bar{B} \rightarrow \ell^-\nu\bar{B}(0.2). \quad (57)$$

Consequently the BR of the LSD signal from the decay of the gluino pair is expected to go up to 3–4%.

Figure 9 shows the expected LSD signal from gluino pair production at LHC for $M_{\tilde{g}} = 300$ and 800 GeV along with the background [21]. The latter comes from $\bar{t}t$ via cascade decay (long dashed) or charge misidentification (dots). Note that the signal is accompanied by a much larger \cancel{p}_T compared to the background because of the LSPs. This can be used to effectively suppress the background while retaining about 1/2 of the signal. Consequently one can search for a gluino up to at least 800 GeV at the low luminosity (10 fb^{-1}) run of LHC, going up to 1200 GeV at the high luminosity (100 fb^{-1}).

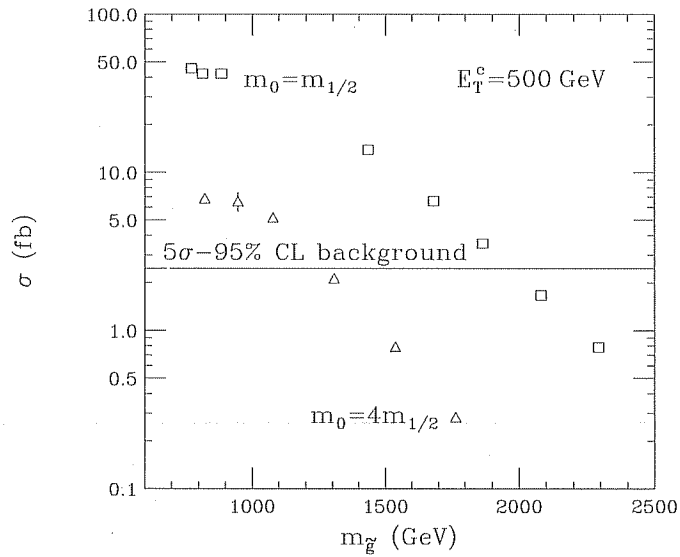


Figure 10. The expected gluino signals at LHC from jets + missing- E_T channel are shown for $M_{\tilde{g}} \simeq M_{\tilde{q}}$ (squares) and $M_{\tilde{g}} \ll M_{\tilde{q}}$ (triangles). The 95% CL background shown also corresponds to $5\sqrt{B}$ for the LHC luminosity of 10 fb^{-1} [22].

Explorable domain of m_0 $m_{1/2}$ parameter space
with 100 fb^{-1} in q, g searches
in n leptons + $E_T^{\text{miss}} + > 2$ jets final states

SUGRA - MSSM, $\tan \beta > 2$, $A_0 = 0$, $\mu < 0$
5 σ contours

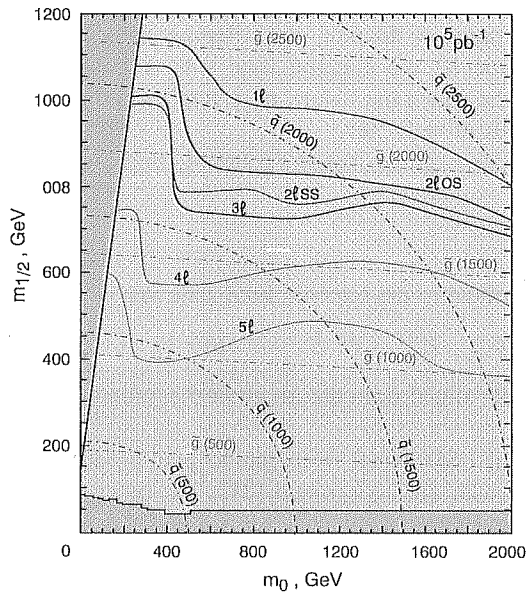


Figure 11. The SUSY discovery limits of various leptonic channels at LHC, where $2l \text{ OS}$ and $2l \text{ SS}$ denote opposite sign and same sign dileptons [13].

Higgs and SUSY searches at LHC

Figure 10 shows the size of the canonical $\cancel{p}_T + \text{jets}$ signal against gluino mass for two cases – $M_{\tilde{g}} \ll M_{\tilde{q}}$ (triangles) and $M_{\tilde{g}} \simeq M_{\tilde{q}}$ (squares) [22]. The background line shown also corresponds to $5\sqrt{B}$ for the LHC luminosity of 10 fb^{-1} . Thus one expects a 5σ discovery limit of at least up to $M_{\tilde{g}} = 1300 \text{ GeV}$ from this signal¹. Finally, figure 11 shows the CMS simulation for the 5σ discovery limits from the various leptonic channels in the plane of $m_0 - m_{1/2}$, the common scalar and gaugino masses at the GUT scale. The corresponding squark and gluino mass contours are also shown. As we see from this figure, it will be possible to extend the squark and gluino searches at LHC well into the TeV region. One should either see these superparticles or rule out SUSY at least as a solution to the hierarchy problem of the SM.

Acknowledgement

The author is thankful to Dr D Denegri of the CMS collaboration for providing figures 7 and 11. He also thanks R S Pawar and S K Vempati for help in plotting figures 1 and 6 and S Datta for embedding the figure files.

References

- [1] For a review see e.g. J F Gunion, H E Haber, G Kane and S Dawson, *The Higgs Hunters' Guide* (Addison-Wesley, Reading, MA, 1990)
- [2] For a review see e.g. H E Haber and G Kane, *Phys. Rep.* **117**, 75 (1985)
- [3] L Maiani, G Parisi and R Petronzio, *Nucl. Phys.* **B136**, 115 (1978)
N Cabbibo, L Maiani, G Parisi and R Petronzio, *Nucl. Phys.* **B158**, 295 (1979)
M Lindner, *Z. Phys.* **C31**, 295 (1986)
- [4] K Riesselmann, hep-ph/9711456 (to appear in Proc. 35th Intl. School of Subnuclear Physics, Erice, 1997) For the theoretical uncertainty in the upperbound see T Hambye and K Riesselmann, *Phys. Rev.* **D55**, 7255 (1997)
- [5] G Altarelli and G Isidori, *Phys. Lett.* **B337**, 141 (1994)
J A Casas, J R Espinosa and M Quiros, *Phys. Lett.* **B342**, 171 (1995); **B382**, 374 (1996)
- [6] LEP Electroweak Working Group and SLD Heavy Flavour Group, CERN-PPE/97-154 (2 December 1997)
- [7] P Janot, *Invited talk at the Indo-French Workshop on Supersymmetry and Unification* (TIFR, Mumbai, 17–21 December 1997)
- [8] M Spira, hep-ph/9705337
- [9] CMS Technical Proposal, CERN/LHCC/94-38 (1994); ATLAS Technical Proposal, CERN/LHCC/94-43 (1994)
- [10] M Dittmar and H Dreiner, *Phys. Rev.* **D55**, 167 (1997)
- [11] For a recent review of radiative correction along with reference to the earlier works see H E Haber, R Hempfling and A H Hoang, *Z. Phys.* **C75**, 539 (1997)
- [12] See e.g. A Djouadi, J Kalinowski and P M Zerwas, *Z. Phys.* **C70**, 435 (1996)
- [13] Simulation study by the CMS collaboration
- [14] D P Roy, *Phys. Lett.* **B277**, 183 (1992); *Phys. Lett.* **B283**, 403 (1992)
S Raychaudhuri and D P Roy, *Phys. Rev.* **D53**, 4902 (1996)
- [15] M Guchait and D P Roy, *Phys. Rev.* **D55**, 7263 (1997)
CDF Collaboration: F Abe *et al.* *Phys. Rev. Lett.* **79**, 357 (1997)
- [16] M Drees, M Guchait and P Roy, *Phys. Rev. Lett.* **80**, 2047 (1998)

¹ This signal may be hard to observe at the high luminosity run due to event pileup.

D P Roy

- [17] E Richter-Was *et al*, CERN-TH-96-111 (1996)
- [18] G L Kane and J P Leville, *Phys. Lett.* **B112**, 227 (1982)
P R Harrison and C H Llewellyn-Smith, *Nucl. Phys.* **B213**, 223 (1983) [Err. *Nucl. Phys.* **B223**, 542 (1983)]
E Reya and D P Roy, *Phys. Rev.* **D32**, 645 (1985)
- [19] W Beenakker, R Hopker, M Spira and P Zerwas, *Nucl. Phys.* **B492**, 51 (1997)
M Kramer, T Plehn, M Spira and P Zerwas, *Phys. Rev. Lett.* **79**, 341 (1997)
- [20] CDF and $D\bar{\phi}$ collaborations: R Culbertson, Fermilab-Conf-97-277-E, Proc. SUSY97 (to be published)
- [21] M Guchait and D P Roy, *Phys. Rev.* **D52**, 133 (1995)
- [22] H Baer, C Chen, F Paige and X Tata, *Phys. Rev.* **D52**, 2746 (1995)